Eva Miglbauer, BSc

Single compartment hydrogen peroxide fuel cells - an organic approach with PEDOT:PSS

MASTER'S THESIS

to achieve the university degree of

Diplom-Ingenieurin

Master's degree programme: Technical Chemistry

submitted to

Graz University of Technology

Supervisor

Assoc.Prof. Dipl.-Ing. Dr.techn., Gregor Trimmel

Institute for Chemistry and Technology of Materials

Eric Daniel Głowacki, PhD
Laboratory of Organic Electronics, Linköping University, Sweden

Graz, October 2018

AFFIDAVIT

I declare that I have authored this thesis independently, that I have not used other than the declared sources/resources, and that I have explicitly indicated all ma- terial which has been quoted either literally or by content from the sources used. The text document uploaded to TUGRAZonline is identical to the present master‘s thesis.

Date

Signature

Abstract

To cope with the increasing demand of clean electrical power sources, new sustainable energy conversion technologies are needed. In this work a novel type of single-compartment fuel cell which uses hydrogen peroxide as both the fuel and the oxidant is investigated. Hydrogen peroxide is outstanding due to a high energy density, its applicability as fuel and as oxidant, and the fact that it is used as an aqueous solution which is easy to store. However, most investigated electrode materials also catalyze the chemical disproportionation of H_2O_2 into H_2O and O_2 leading to a decrease of performance of the fuel cell. Also, the stability over time of such fuel cells has not been evaluated. Therefore, new catalyst materials are examined, which mitigate the loss of hydrogen peroxide as fuel and are evaluated for longer-term operation. In this context, the conducting polymer poly(3,4-ethylenedioxythiophene) (PEDOT) shows promising properties, since it is easy to process and forms a three-dimensional conducting hydrogel in water. The best performance was reached with a PEDOT:PSS (poly(styrene sulfonic acid)) free-standing foil as cathode and a Ni-mesh as anode. A high open circuit potential of 0.55 V and a power density of 0.3 mW cm^{-2} was obtained with 0.1 M H_2O_2.

Kurzfassung

Um die ansteigende Nachfrage nach sauberer Stromversorgung zu bewältigen, müssen neue und nachhaltige Technologien für die Energieumwandlung entwickelt werden. Deshalb wird in dieser Arbeit eine neuartige Form einer Brennstoffzelle untersucht. Bei dieser Einzelkammer-Brennstoffzelle wird Wasserstoffperoxid als Brennstoff und als Oxidationsmittel verwendet. Wasserstoffperoxid sticht durch die hohe Energiedichte, die Eignung als Brennstoff und als Oxidationsmittel und die leichte Lagerung, da es als Flüssigkeit vorliegt, hervor. Fast alle, bis jetzt untersuchten Elektrodenmaterialien haben den Nachteil, dass sie auch die chemische Disproportionierung von H_2O_2 zu H_2O und O_2 katalysieren, was eine Minderung der Leistung nach sich zieht. Weiters ist wenig über die Langzeitstabilität solcher Systeme bekannt. Deshalb werden in dieser Arbeit neue Katalysatormaterialien untersucht, die den Verlust an Wasserstoffperoxid vermindern. Diese werden auch nach ihrer Langzeitstabilität beurteilt. Unter diesen Gesichtspunkten zeigt das leitende Polymer Poly(3,4-ethylendioxythiophen) (PEDOT) verheißungsvolle Eigenschaften. Es erlaubt eine leichte Verarbeitbarkeit und die Bildung eines drei dimensionalem leitenden Hydrogel in Wasser. Die beste Leistung wurde mit einer freistehenden Folie aus PEDOT:PSS (Polystyrolsulfonsäure) als Kathode und einem Ni-Netz als Anode erreicht. Bei offenem Stromkreis wurde ein Potential von 0.55 V und eine Leistungsdichte von 0.3 mW cm^{-2} mit 0.1 M H_2O_2 erreicht.

Acknowledgements

I would like to thank my supervisor at the TU Graz Gregor Trimmel for accepting me as his Master student and therefore giving me the opportunity to go abroad and gain precious experience concerning science and life.
I owe special thanks to my supervisor at Linköping University, Eric Daniel Glowacki. He always gave me valuable advice and guidance through the whole process of my thesis. Moreover, he provided me with new input and ideas when it got challenging. I also want to show my appreciation for his patience, the opportunities and inspiring environment he created.
I would like to express my gratitude as well to Magdalena Warczak, Maciej Gryszel, Vedran Derek and many other colleagues of the Laboratory of Organic Electronics for their friendly ear, teaching me specific techniques, their support and help with scientific problems.
Finally, I want to say thank you to my family and friends for their support through my whole time of study, for their encouragement and patience.

Table of Contents

1. Introduction

Since the worldwide demand for energy is increasing it is important to find solutions for "green" and clean production and storage of energy which are carbon neutral, i.e. not increasing the net release of CO_2.[1]

In this context fuel cells are a promising technology for storage and generation of electricity from carbon free sources. The most frequently investigated and developed fuel cell is the hydrogen fuel cell, where hydrogen gas gets oxidized to H^+ at the anode while oxygen is reduced at the cathode to OH^-. Electrical power is produced and the net product is water.[2] However, conventional H_2 fuel cells have drawbacks, mainly concerning storage and transportation of hydrogen, which is a flammable gas.[3] Moreover, polymer electrolyte fuel cells, one of the most common types, require Pt as catalyst, which is one of the most expensive noble metals. These drawbacks motivate the exploration of new technologies, which are cheap in production, with non-toxic materials and chemicals, have a small CO_2 footprint and show efficient power conversion.[1]

Hydrogen peroxide (H_2O_2) is a highly energetic fuel since it can spontaneously decompose to water and oxygen, two highly-stable products. In contrast to hydrogen, it forms a stable aqueous solution. High energy density and ease of storage make it a promising fuel.[4,5] Moreover, it can even be applied as oxidant and therefore no membrane for the separation of the cathode and anode chamber is necessary, making engineering of the hydrogen peroxide fuel cell simpler.[5]

In this work, new catalyst materials for single compartment hydrogen peroxide fuel cells are investigated.

1.1. Hydrogen peroxide

Hydrogen peroxide, with the chemical formula H_2O_2, is a clear and colorless liquid. It is miscible with water, independent of the respective amount, and weakly acidic in aqueous solutions (acid dissociation constant of $1.78 * 10^{-12}$ at 20 °C). In addition, it can behave as an oxidizing or reducing agent depending on the redox potential of the reacting species and the pH of the environment.[4]

Hydrogen peroxide is a molecule with a wide range of applications. For example, it is used as a bleaching agent in the textile industry, the paper and pulp production as well as for hair coloring. Additionally, hydrogen peroxide is employed for the synthesis of several chemicals as well as an oxidizing agent. Since it has disinfectant properties it

is also used in medical applications and waste water treatment. Moreover, due to the high energy density it is utilized as rocket fuel.[4] A novel emerging application of hydrogen peroxide is as fuel and as oxidant in fuel cells.[2]

Hydrogen peroxide was synthesized for the first time by L. J. Thenard, who used barium peroxide with nitric acid to create the peroxide. Later, Meidinger found a new process route where it was produced by electrolysis of sulfuric acid and subsequent hydrolysis. Nowadays, the most frequently used process is the organic autooxidation process. In this method 2-alkyl-9,10-anthraquinone is reduced with H_2 and the help of a catalyst followed by oxidation with O_2 where hydrogen peroxide is formed. This was the move towards large scale production.[4] However, the required H_2 is usually obtained by steam reforming of natural gas where also a high amount of CO_2 is generated.[6] Therefore more environmentally friendly and less energy demanding methods like photocatalytic and electrochemical production on semiconductor materials from O_2 and H_2 or water are currently examined.[6–10]

1.2. Hydrogen peroxide fuel cells

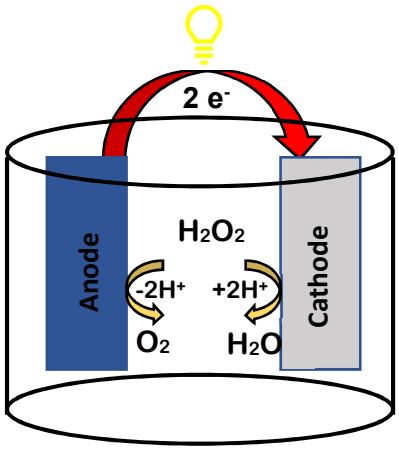

Figure 1: Scheme of a single compartment hydrogen peroxide fuel cell

Single compartment hydrogen peroxide fuel cells are a novel fuel cell type standing out with a simple design. Figure 1 shows a basic schematic of the peroxide fuel cell. They do not need a membrane to separate cathode and anode since hydrogen peroxide takes part as fuel and as oxidant and selective electrodes for reduction and oxidation can be applied. This greatly simplifies the design, thus potentially low cost fuel cells can be developed.[5]

Hydrogen peroxide itself is a carbon-free energy carrier, the only decomposition products are water and O_2. Hence, a carbon free energy supply is assured. Moreover, since hydrogen peroxide is liquid and soluble in water, simple storage and

transportation of the fuel is possible. Additionally, basic and acidic environment can be applied.[5,11]

Hydrogen peroxide can be produced via photoelectro- or electrocatalysis with low energy consumption and then used for energy generation.[3,9,12]

The basic principle of this type of fuel cell is the reduction of hydrogen peroxide to water at the cathode (equation 1) as well as oxidation to O_2 at the anode (equation 2).[5] A theoretical open circuit potential of 1.09 V can be achieved, which is comparable to a hydrogen fuel cell (1.23 V) or a direct methanol fuel cell (1.21 V).[13]

Reaction equations of a hydrogen peroxide fuel cell: [5,13]

Cathode:	$H_2O_2 + 2H^+ + 2e^- \rightarrow 2\ H_2O$	(0.682 V vs NHE)	(1)
Anode:	$H_2O_2 \rightarrow O_2 + 2H^+ + 2e^-$	(1.77 V vs NHE)	(2)
Total:	$2\ H_2O_2 \rightarrow 2\ H_2O + O_2$	(1.09 V)	(3)

Single compartment hydrogen peroxide fuel cells were first developed by Yamazaki et al. They applied Ag as the cathode and Au, Pt, Pd or Ni as anode in alkaline media. With Pt as anode the highest current was achieved but also the highest amount of oxygen bubbles, caused by decomposition of peroxide without electricity generation, appeared. With this drawback in mind Ni seemed to be the best solution since it has the lowest decomposition rate and moreover it is the cheapest metal of the tested ones. However, Ni gave the lowest currents in this experiment.[5]

Yamada et al. designed a fuel cell with a Ag/Ag-Pb alloy composite electrode as cathode and Au as anode in basic media. A maximum power density of 0.075 mW cm^{-2} at 0.065 V and only an open circuit potential (V_{OC}) of 150 mV was demonstrated.[12]

With Prussian blue coated on carbon as cathode and Ni or Ag as anode in acidic media a maximum power density of 1.55 mW cm^{-2} and an V_{OC} of 0.6 V was reached.[11]

The highest power density of 4.2 mW cm^{-2} was reported by Yamada et al.[14] They used a carbon supported pyrazine bridged $Fe[Me(CN)_4]$ complex as cathode and Ni as anode whereas as Me Pt or Pd ions were utilized. Also, V_{OC} values between 0.7 and 0.8 V were achieved. To-date, organic semiconductors have not been explored as catalysts in hydrogen peroxide fuel cells.

1.3. Catalyst materials

1.3.1. Poly (3,4-ethylenedioxythiophene)

Poly(3,4-ethylenedioxythiophene) or PEDOT is an organic semiconducting polymer, which can be highly conductive if doped. In Figure 2 the chemical structure of PEDOT is illustrated. It was first synthesized at the Bayer AG research laboratories by standard oxidative chemical or electrochemical polymerization from the monomer ethylenedioxythiophene (EDOT). To increase the solubility and to counterbalance the positive charge of doped PEDOT, a water-soluble anionic polyelectrolyte, poly(styrene sulfonic acid), also called PSS, was used.[15,16] The chemical structure of PSS is shown in Figure 2. Properties of PEDOT:PSS which make this compound superior are, as already mentioned, the high conductivity as well as the stability and the easy processability.[17]

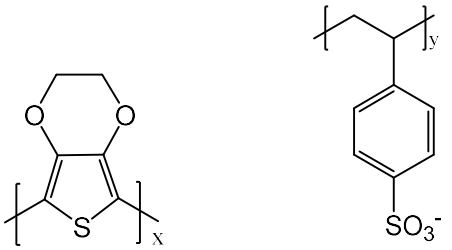

Figure 2: Chemical structure of PEDOT (left) and PSS (right)

Applications of PEDOT are for example as antistatic coating for plastics or photographic films, as electrode material for solid electrolyte capacitors or in photovoltaic devices.[15,16] Moreover, it is also an electrocatalyst for the oxygen reduction reaction (ORR).[18,19] There are many more applications which can be found in several reviews.[15,16,20] Howsoever, it is already reported as composite electrode with various materials for hydrogen peroxide sensing.[21–23] In this work PEDOT:PSS is applied as cathode material for hydrogen peroxide fuel cells with and without additional incorporation materials like prussian blue, alizarin and lignosulfonate.

1.3.2. Prussian Blue

Prussian blue (PB) or ferric ferricyanide $(Fe_4[Fe(CN)_6])_3$ is a long known coordination complex with a dark blue color.[24] As discussed in section 1.2, PB was already used as a catalyst material for hydrogen peroxide fuel cells as well as for hydrogen peroxide sensors in bio applications.[11,21,24,25] PB is known to be highly selective to hydrogen peroxide reduction and also more active towards the reduction reaction compared to

Pt.[26] However, hydroxyl ions can dissolve PB and therefore it is only stable in acidic media.[26,24]

Prussian blue can be synthesized chemically and electrochemically, which can also be applied for thin film deposition.[11,21,24]

1.3.3. Catechol derivatives

Catechol or 1,2-dihydroxybenzene is an organic compound, which is easy to oxidize.[27] The idea is that hydrogen peroxide oxidizes the two hydroxy groups attached to the aromatic ring while hydrogen peroxide itself gets reduces. The redox reaction is shown in Figure 3. Two compounds with this kind of functional group are alizarin and lignosulfonate.

Oxidation of catechol:

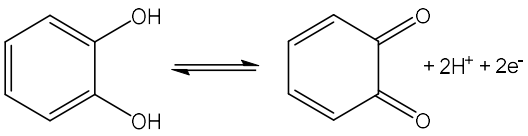

Figure 3: Redox reaction of 1,2-dihydroxybenzene or catechol to 1,2-benzoquinone, reproduced from [28]

1.3.3.1. Alizarin

Alizarin, alizarin red or 1,2-dihydroxyanthraquinone is a red pigment used as organic dye, for analytical chemistry or in medical applications, to name a few utilizations.[29] It is an anthraquinone derivative with a catechol group, the structure can be seen in Figure 4.

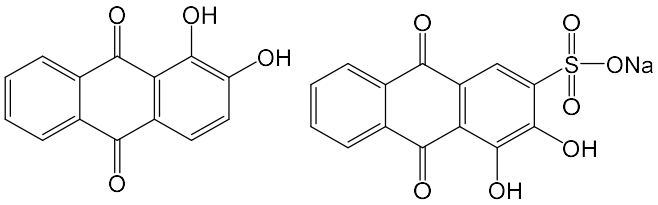

Figure 4: Chemical structure of alizarin (left) and alizarin red S (right)

Alizarin red S, an alizarin derivate sulfonated on position 3, whereas the sulfonate group is responsible for better solubility but inactive concerning reactivity, is already used for hydrogen peroxide sensors in composite materials.[30,31]

1.3.3.2. Lignosulfonate

Lignosulfonate (LS) is synthesized from lignin, the second most copious biopolymer. Lignin itself is a byproduct in paper and pulp production and therefor an inexpensive material. LS is irregular in structure, containing phenylpropane groups, hydrophilic sulfonic groups and electroactive methoxyphenol groups.[32] Ajjan et al. suggested a

synthetic pathway for electropolymerization of EDOT with lignin to PEDOT/LS composite materials, whereas LS acts as dispersing agent as well as dopant. The proposed reaction scheme is shown in Figure 5.[33]

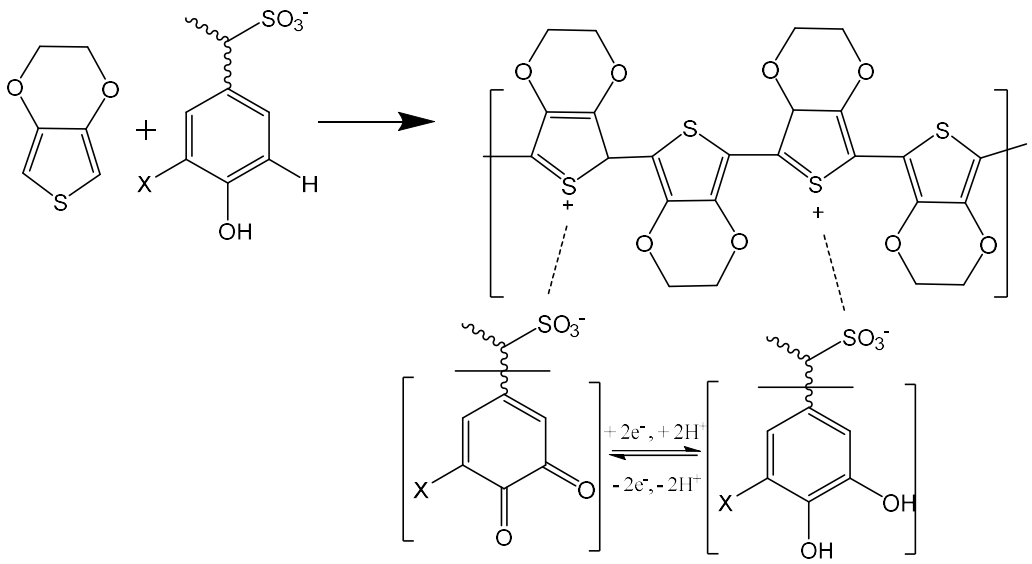

Figure 5: Electrochemical synthesis of PEDOT/LS, according to [33]

Moreover, Edberg et al. successfully integrated LS into solution processed PEDOT:PSS, which enables easy and large volume processability.[34]

1.3.4. Nickel

Nickel is a non-noble transition metal with the atomic number 28. As mentioned above, it was already applied as anode material for single compartment hydrogen peroxide fuel cells.[5,11,14] Unfortunately, Yamazaki et al. reported that disproportionation of peroxide occurs at nickel surfaces. Nevertheless, the disproportionation rate is lower compared to Pt, Pd, Ag or Au although the generated power, compared to these metals, is lower as well.[5]

2. Experimental

2.1. Materials

All used chemicals and materials are depicted in Table 1.

Table 1: Overview of used chemicals and materials

Material/Compound	Supplier	Purity	Referred to
Indium tin oxide	Kintek ltd	-	ITO
Fluorinated tin oxide	Ossila	TEC-15	FTO
Carbon black on polyethylene	prepared in-house by Pawel Wojcik	-	Printed Carbon
Gold/Chromium/Glass substrate	Prepared in-house by Magdalena Warczak	-	Au substrate / Au
Nickel-mesh	Aldrich	-	Ni
Platinum Rhodium gauze	Alfa Aesar	-	Pt
Hellmanex III	Hellma analytics	-	-
Acetone	Solveco	≥ 99.5%	
Isopropanol	Solveco	-	
Potassium ferricyanide	Sigma Aldrich	≥ 99.0 %	$K_3[Fe(CN)_6]$
Iron(III)chloride hexahydrate	Sigma Aldrich	≥ 99.0 %	$FeCl_3 * 6\ H_2O$
Hydrochloric Acid	VWR Prolab Chemicals	37 %	HCl
Clevios PH 1000	Heraeus	-	poly(3,4-ethylenedioxythiophene): poly(styrene sulfonate), PEDOT:PSS
Dimethylsulfoxide	Sigma Aldrich	≥ 99.9 %	DMSO
(3-Glycidoxypropyl)-trimethoxysilane	Alfa Aesar	97 %	GOPS
Nanofibrillated cellulose	Prepared in-house by Jesper Edberg	0.52%	NFC
Ethanol	VWR Prolab Chemicals	100 %	EtOH
1,2-Dihydroxy-anthraquinone	Aldrich	-	Alizarin
Lignosulfonate	MeadWestvaco	-	LS

Hydrogen Peroxide	Sigma Aldrich	30 wt%	H_2O_2, peroxide
Argon	Linde	-	Ar
Oxygen	Linde	-	O_2
3,4-Ethylenedioxythiophene	Aldrich	97 %	EDOT
Acetonitrile	VWR Prolab Chemicals	≥ 99.5%	-
Perchloric acid	Sigma Aldrich	70 %	$HClO_4$
Sodium phosphate dibasic	Sigma Aldirch	≥ 99.0 %	Na_2HPO_4
Citric acid, monohydrate	VWR Prolab Chemicals	99 – 102 %	$HOC(COOH)(CH_2COOH)_2 \cdot H_2O$
Horseradish peroxidase	Aldrich	-	HRP
3,3′,5,5′-Tetramethylbenzidine	Aldrich	-	TMB
Tetracyanoquinodimethane	TCI	≥ 99.0 %	TCNQ
4-dicyanomethylene-2-p-tolyl-6-phenyl-4H-thiopyran-1,1-dioxide	Kodak	-	SA-3
N,N′-Dioctyl-3,4,9,10-perylenedicarboximide on Au substrate	Prepared in-house by Magdalena Warczak	-	PTCDI
Quinacridone on Au substrate	Prepared in-house by Magdalena Warczak	-	QNC
Iron(II,III) hexacyanoferrate(II,III)	-	-	Prussian Blue, PB
poly(3,4-ethylene-dioxythiophene) perchlorate	-	-	PEDOT/ClO_4^-

2.2. Catalyst preparation for incorporation

2.2.1. Prussian Blue

Prussian Blue (PB) synthesis was carried out according to the works of Moushavi Shaegh et al. and Wang et al.[11,21] In brief 10 mL of 0.5 M $FeCl_3$ * 6 H_2O in 0.1 M HCl was added dropwise to 10 mL of 0.5 M $K_3[Fe(CN)_6]$ in 0.1 M HCl and then stirred for 1.5 h. After addition of acetone the dispersion was centrifuged at 10000 rpm for 10 minutes. Then the precipitate was washed with ethanol and again centrifuged. Afterwards, it was washed and centrifuged with 18 MΩ H_2O twice and then dried overnight at 80 °C.

2.3. Substrate preparation

2.3.1. ITO and FTO

ITO and FTO substrates were cleaned by consecutive ultrasonication for 10 minutes in a detergent solution (Hellmanex 5% solution), 18 MΩ H_2O, acetone and isopropanol. After drying with high pressure air, the samples were cleaned for 15 minutes with a Novascan Ozone cleaning device, model PSD-UV8.

2.3.2. Au and printed Carbon

The cut substrates were cleaned for 15 minutes with a Novascan Ozone cleaning device, model PSD-UV8.

2.4. Electrode preparation

All electrochemical preparation methods were performed with a Keithley Sourcemeter 2450.

2.4.1. Electrodeposited Prussian Blue on ITO

The synthesis was based on the work of García-Jareño et al.[35] Two solutions were prepared: 0.05 M $FeCl_3$ * 6 H_2O in 0.05 M HCl and 0.05 M $K_3[Fe(CN)_6]$ in 0.05 M HCl. Before deposition, 5 mL of 0.05 M HCl was mixed with 10 mL of each solution. The substrate was immersed into the liquid and connected as working electrode. A Pt mesh was functionalized as counter electrode. -150 µA cm^{-2} for 120 s were applied. Afterwards the electrodes were rinsed with water and dried with pressurized air.

2.4.2. PEDOT:PSS - GOPS

The preparation of the solutions was based on the work of Håkansson et al.[36] DMSO was added to increase the conductivity.[17]

2.4.2.1. Foil

20 mL of Clevios PH 1000 was mixed with 2 vol% DMSO and 0.5 vol% GOPS and afterwards ultrasonicated for 10 minutes. Then the mixture was poured into a Petri dish (diameter of 8.5 cm) and stored under the fume hood overnight. Afterwards it was dried at 80 °C in the oven for two hours. The obtained foil was removed from the Petri dish. The foil was cut into suitable pieces for electrodes.

2.4.2.2. Drop casting on FTO

For drop casting 20 mL of Clevios PH 1000 was mixed with 2 vol% DMSO and 0.5 vol% GOPS and afterwards ultrasonicated for 10 minutes. Afterwards a defined volume of the solution was drop cast on a defined area of cleaned FTO substrates and annealed for 20 minutes on a heating plate at 120 °C.

2.4.3. PEDOT:PSS – NFC

The preparation of the solution was based on the work of Malti et al.[17]

2.4.3.1. Foil – original recipe

4.7 g of Clevios PH 1000 solution were mixed with 4.4 g of 0.52 wt% aqueous nanofibrillated cellulose (NFC) and 258 mg DMSO with the help of an ultra-turrax for several minutes. Afterwards the solution was poured into a Petri dish (diameter of 5.3 cm) and dried for 48 hours under the fume hood. Then it was dried at 80 °C for two hours. The foil was removed from the Petri dish. The foil was cut into suitable pieces for electrodes.

2.4.3.2. Foil – 1.5 times higher amount of Clevios PH 1000

The above mentioned original recipe was increased to a 1.5 times higher amount of Clevios PH 1000.

2.4.3.3. Drop cast on FTO

4.7 g of Clevios PH 1000 solution were mixed with 4.4 g 0.52% aqueous nanofibrillated cellulose (NFC) and 258 mg DMSO with the help of an ultra-turrax for several minutes.

Afterwards a defined volume of the solution was drop cast on a defined area of cleaned FTO substrates and annealed for 20 minutes on a heating plate at 120 °C.

2.4.4. Electropolymerized PEDOT/ClO_4^-

The synthesis was based on the work of Ajjan et al.[33] Electropolymerization of PEDOT/ClO_4^- was performed on pC and Au in 10 mM EDOT in 0.1 M $HClO_4$/Acetonitrile (9:1) vs Pt. A current density of 0.25 mA cm^{-2} for 300, 600 and 900 s was applied.

Also, electropolymerized LS/PEDOT was synthesizes as mentioned above with the only difference that 1 mg mL^{-1} LS was added to the electrolyte.

Electropolymerization of PEDOT on FTO was performed in a solution of 50 mM EDOT in 50 mM $HClO_4$ at 1.25 V for 90 s.

2.4.5. Incorporation of catalyst into PEDOT:PSS – NFC

About 12.5 mg of catalyst (Prussian Blue, alizarin or lignosulfonate) was dissolved or dispersed in 5 mL of 18 MΩ H_2O and ultrasonicated for 10 minutes. Then 4.7 g of Clevios PH 1000 solution, 4.4 g of 0.52 wt% aqueous NFC and 258 mg DMSO were added and mixed with an ultra-turrax for several minutes. To avoid accumulation of insoluble catalyst on the surface, a small amount of ethanol was added. Afterwards the solution was poured into a Petri dish (diameter of 5.3 cm) and dried for 48 h under the fume hood. Next the almost solid foil was dried at 80 °C for two hours. The foil was removed from the Petri dish.

2.4.6. Surface oxidation of Ni (oxidized Ni)

A Ni mesh was placed into a Protherm tube furnace ASP 11/70/750-3Z and heated for 15 minutes at 500 °C.

2.4.7. 4-dicyanomethylene-2-p-tolyl-6-phenyl-4H-thiopyran-1,1-dioxide (SA-3)

2 wt% of SA-3 were dissolved in acetone. 50 µL of the solution was drop cast on printed carbon and dried at room temperature.

2.4.8. Tetracyanoquinodimethane (TCNQ)

TCNQ was sublimated onto a FTO substrate under vacuum at 140 °C in a Protherm tube furnace ASP 11/70/750-3Z.

2.4.9. Oxidized Ti

A Ti sheet was immersed into a mixture of 40 mL of 30 wt% hydrogen peroxide, 5 mL of 2 M HCl and 10 mL of 18 MΩ H_2O for 10 minutes. Afterwards, it was placed into a Protherm tube furnace ASP 11/70/750-3Z at 480 °C for one hour.

2.5. Further preparation of electrodes

To avoid wetting of the crocodile clips, in case of the PEDOT foils, and to define the electrode area a Kapton tape was applied. To make sure of conducting connections with the crocodile clips a copper tape was attached to the top of the electrodes.

2.6. Electrochemical Characterization

All electrochemical measurements were performed with a Keithley Sourcemeter 2450. Step chronopotentiometry and open circuit potential measurements were performed with an Ivium Vertex One potentiostat/ galvanostat.

2.6.1. Catalyst examination

All potential electrode materials were tested in a single compartment fuel cell set up, which consisted of working and counter electrode in a beaker filled with 15 mL of electrolyte. The measurements were performed in a cyclic voltammetry mode, the scan range was from 0 to 0.8 V with a scan rate of 50 mV s^{-1}. In the case of cathode materials the counter electrode was a Ni-mesh, in the case of anode materials the applied cathode electrodes were electrodeposited Prussian blue on ITO or PEDOT:PSS – GOPS.

First, measurements were conducted in 0.05 M HCl without peroxide (WO). Then measurements in 0.05 M HCl with 0.1 M H_2O_2 (W) were done. For Au samples 0.033 M H_2SO_4 was used as supporting electrolyte instead of HCl. Several measurements were recorded until stable cycles were obtained.

2.6.2. Open circuit potential and Step-Chronopotentiometry

The open circuit potential (V_{OC}) measurements and step chronoamperometry were performed with an Ivium Vertex One potentiostat/ galvanostat. A single compartment fuel cell with the examined electrode as cathode and a Ni-mesh as anode was filled with 15 mL of 0.1 M H_2O_2 in 0.05 M HCl. The V_{OC} was measured at 0 mA, whereas for the step chronoamperometry several steps at different currents were applied (see Table 2 and Table 3).

Table 2: Applied steps for chronopotentiometric measurements of PEDOT:PSS – NFC and PB/PEDOT:PSS - NFC

Current / mA	Time / s	Current / mA	Time / s
0.00	120	-1.00	80
-0.05	80	-1.25	80
-0.10	80	-1.50	80
-0.20	80	-1.75	80
-0.40	80	-2.00	80
-0.60	80	-2.25	80
-0.80	80	-2.50	80

Table 3: Applied steps for chronopotentiometric measurements of PEDOT:PSS - GOPS

Current / mA	Time / s	Current / mA	Time / s
0.00	120	-1.75	80
-0.05	80	-2.00	80
-0.10	80	-2.25	80
-0.20	80	-2.50	80
-0.40	80	-2.75	80
-0.60	80	-3.00	80
-0.80	80	-3.25	80
-1.00	80	-3.50	80
-1.25	80	-3.75	80
-1.50	80	-4.00	80

2.6.2. Chronoamperometry

Chronoamperometric measurements were performed in a single compartment fuel cell set up, as described above. For several hours, 0 V vs Ni were applied. As electrolyte 15 mL of 0.1 M H_2O_2 in 0.05 M HCl was used.

2.6.3. Purging experiments – cyclic voltammetry

Cyclic voltammetry was performed under saturated argon atmosphere, ambient conditions and saturated O_2-atmosphere. Therefore, the sealed and assembled single compartment fuel cell with 10 mL of electrolyte was purged for one hour before starting the measurements in case of Ar and O_2. First, measurements were conducted in 0.05 M HCl without peroxide (WO). Then measurements in 0.05 M HCl with 0.1 M H_2O_2 (W) were done. Therefore, the needed amount of peroxide was injected with the help of a syringe and purged for another 10 minutes. Scan range was from -0.4 V to 0.8 V with a scan rate of 5 mV s^{-1}.

2.7. Hydrogen peroxide assays

2.7.1. UV vis – direct assay

The measurements were done with an absorption spectrometer Perkin Elmer Lambda 900. Electrode materials were immersed in 0.05 M H_2O_2 in 0.05 M HCl. Every hour over six hours 3 mL of each sample solution were taken and absorption spectra were recorded from 200 to 300 nm. After measuring, the taken amount was mixed again with each sample solution. To obtain the resulting hydrogen peroxide concentration, the measured optical density (*OD*) values at 240 and 250 nm were taken from the spectra and the corresponding concentration values were extracted from the calibration line in Figure 6.

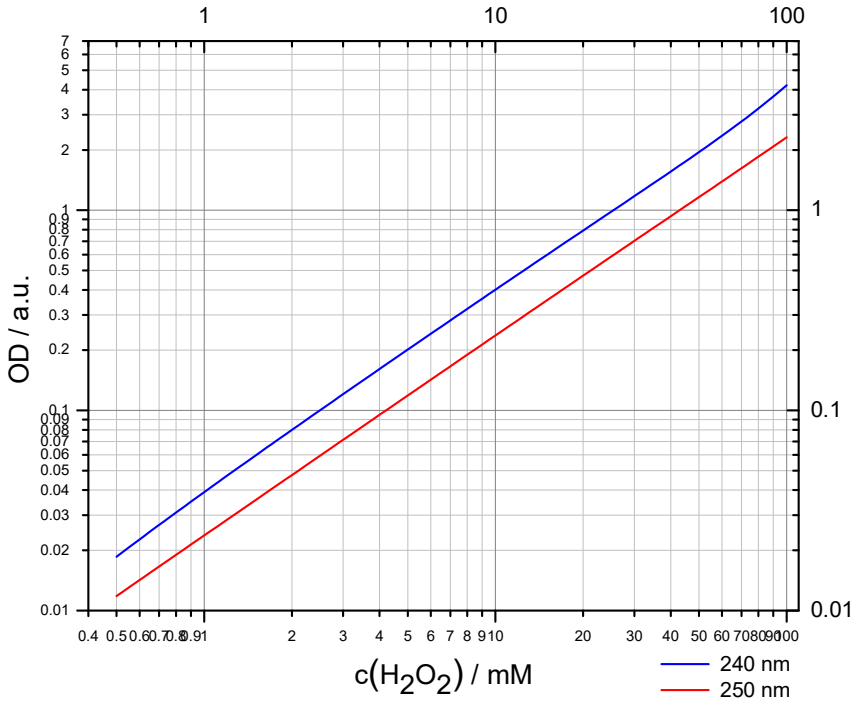

Figure 6: Calibration curve for direct UV-vis assay, optical density OD vs concentration of peroxide for 240 and 250 nm

2.7.2. HRP/TMB assay

The HRP/TMB assay was done after a method described by Jakešová et al.[7]
First, 99.3 vol% of a buffer solution, containing 0.4 M Na_2HPO_4 and 0.2 M citric acid in a ratio of 10:7 with a pH of 5.52, were mixed with 0.2 vol% HRP and 0.5 vol% TMB. For the measurement, each electrode material was immersed in 10 mL of 0.03 M H_2O_2 in 0.05 M HCl. Every hour for the duration of five hours 50 µL of each sample solution were taken and tenfold dilutions with 0.05 M HCl were prepared. 30 µL of each dilution were mixed with 270 µL of the above-mentioned mixture and measured at 653 nm with a BioTek Synergy H1 Hybrid Multi-Mode Reader. The concentration of peroxide was determined by using the obtained extinction coefficient of the TMB dimer and validated with the help of a calibration curve. For calibration, solutions with known hydrogen peroxide concentration of 0, 10, 20, 30 and 40 µM were measured.

3. Results and Discussion

3.1. Catalyst examinations – Cathode

To compare different cathodic catalyst materials in a H_2O_2 fuel cell geometry, cyclic voltammetry was performed as a first experiment. The method was chosen because it is fast and easy to conduct. A Ni-mesh was used as counter electrode as it is an established catalyst for peroxide oxidation.[5,11,14] Over the course of multiple experiments, due to corrosion, the nickel mesh was replaced several times.

As supporting electrolyte, 0.05 M HCl was chosen, since it was already used in existing literature and H_2O_2 is more stable in acidic media than in basic one.[2,11] To see if the material reacts with the hydrogen peroxide and not with the electrolyte itself always two voltammograms were measured, without (WO) and with 0.1 M H_2O_2 (W), where the needed amount of peroxide was added to the electrolyte after the first voltammetric measurement.

In a fuel cell performance test, only linear sweep measurements are conducted. Therefore, only the half scan from 0.8 to 0 V, which is always the sweep near the abscissa, is relevant for comparison and extraction of the open circuit potential (V_{OC}). The determined currents were normalized by dividing them with the electrode area. In the case of PEDOT-foils it was divided by two times the area, since front and back side are considered active area. Since the PEDOT:PSS foil swells in electrolyte, in reality the actual functional area is most likely larger, however it is not possible to precisely quantify this, therefore all current densities were referenced to the two-dimensional areas of the front and back of the electrode.

3.1.1. Electrodeposited Prussian blue (PB) on ITO (cathode) vs Ni anode

Since PB has been reported as a promising peroxide reduction catalyst, PB cathodes were used as a comparative benchmark. PB was electrodeposited on ITO and tested as a cathode (Figure 7). With a peroxide concentration of 0.1 M, a short circuit current density j_{SC} of 7 mA cm^{-2} was reached which is 2 mA cm^{-2} lower compared to PB on carbon. However, for V_{OC} the same value of 0.6 V was obtained.[11]

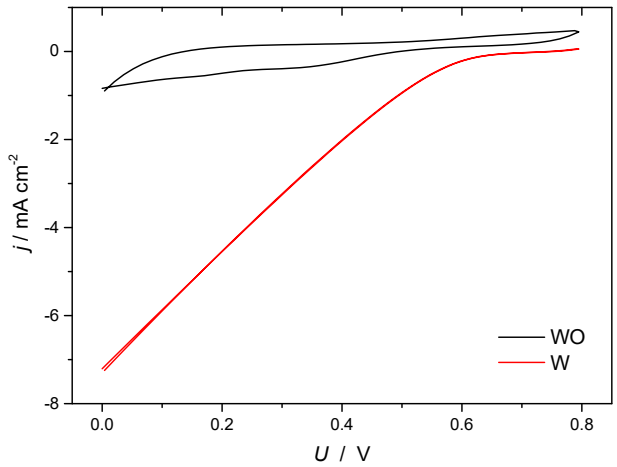

Figure 7: Cyclic voltammogram of electrodeposited PB on ITO vs Ni, 0.05 M HCl without (WO) and with 0.1 M hydrogen peroxide (W)

3.1.2. PEDOT:PSS - GOPS

PEDOT:PSS - GOPS was prepared as drop-cast film on printed carbon (pC) and on FTO as well as freestanding foil. GOPS was added as a crosslinking agent to avoid dissolution and delamination of the film in aqueous solutions.[36] The amount of PEDOT:PSS solution which was used in the preparation of the electrodes varied for the different types of samples. To compare the following results, it is useful to define the electrodes in terms of PEDOT:PSS volume per area of the electrode. These values are compared in Table 4.

Table 4: Used amount of PEDOT:PSS - GOPS solution for electrode preparation

Preparation method	Volume per electrode area / µL cm^{-2}
drop-cast on pC	357
drop-cast on FTO	182
foil	272

In Figure 8 the cyclic voltammetry scans of all three differently prepared PEDOT:PSS - GOPS electrodes are depicted. All show similar behavior without peroxide. However, with 0.1 M peroxide the foil performs best for the reduction reaction of peroxide with a j_{SC} of -3.5 mA cm^{-2} and an V_{OC} of 0.5 V.

The printed carbon electrode appears to have the lowest activity towards reduction, although the highest amount of PEDOT:PSS solution was used. Only an V_{OC} of 0.4 V and a j_{SC} of -2.25 mA cm^{-2} were reached. Moreover, after measurements, the drop cast PEDOT:PSS as well as the printed carbon delaminated from the PE foil.

The short circuit current density of PEDOT:PSS – GOPS on FTO is only -0.25 mA cm^{-2} higher than for pC. Yet, the V_{OC} is similar to the foil. The advantage of the drop cast PEDOT on FTO compared to the foil is, that the resistance increase quantified with an ohmmeter after cyclic voltammetry measurements was lower.

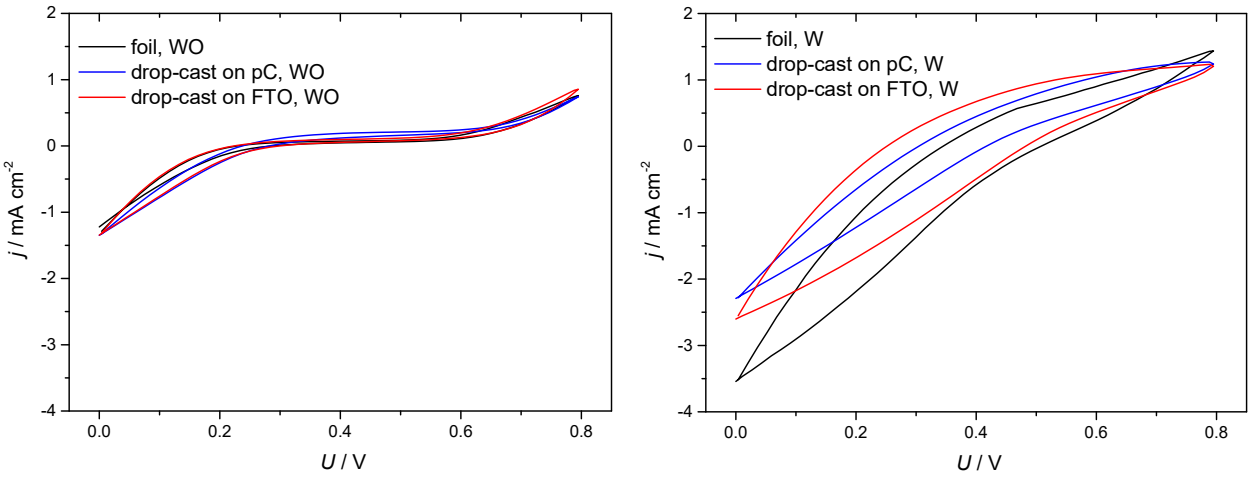

Figure 8: Cyclic voltammogram of PEDOT:PSS - GOPS drop cast on printed Carbon (pC), on FTO (FTO) and as foil vs Ni: left: 0.05 M HCl without peroxide (WO) ; right: 0.05 M HCl with 0.1 M peroxide (W)

3.1.3. PEDOT:PSS - NFC

To maintain the conductivity and stability of PEDOT:PSS, nanofibrilated cellulose (NFC) was added instead of GOPS.[17] Two different foils, one of them with a 1.5 times higher amount of PEDOT solution, and a drop cast film on FTO were prepared.

The drop cast film delaminated quickly while immersed into the electrolyte. Therefore, no further examinations were done.

The results are presented in Figure 9. Since the original recipe, compared to the GOPS foil, contains a smaller amount of Clevios PH 1000 the achieved current densities are lower. For this reason, a foil with a higher amount of Clevios PH 1000 solution, but still lower than for GOPS, was prepared. The current densities increased, but they are still 1 mA cm^{-2} lower than achieved with GOPS foils. However, the obtained V_{OC} is 0.6 V, which is comparable to PB on ITO (see Figure 7).

In general, PEDOT:PSS – NFC foils are less brittle than those with GOPS. Nevertheless, the swelling effect during immersion into a liquid is higher.

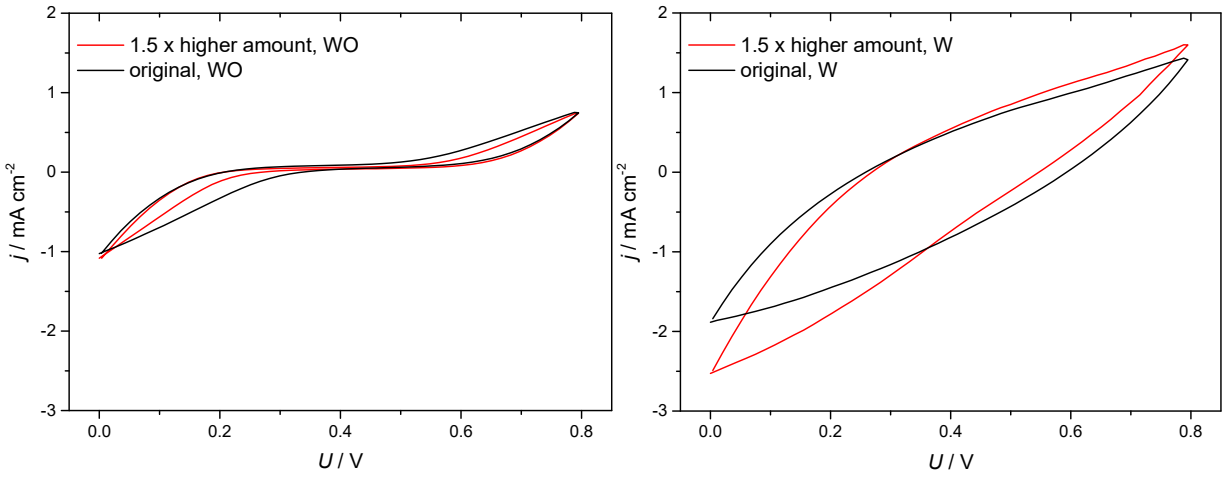

Figure 9: Cyclic voltammogram of PEDOT:PSS - NFC vs Ni; left: 0.05 M HCl without peroxide (WO); right: 0.05 M HCl with 0.1 M peroxide (W)

3.1.4. Incorporation with PEDOT:PSS – NFC

Three different composite materials as freestanding foils with PEDOT:PSS - NFC were prepared – PB, Alizarin and lignosulfonate (LS). To avoid crosslinking of catalyst materials with GOPS, PEDOT:PSS - NFC was chosen as matrix.

Alizarin and PB are not soluble in water. Hence, it was difficult to obtain a well distributed foil, since the particles agglomerated during drying.

In Figure 10 the different composite materials are compared to PEDOT:PSS - NFC without any incorporation and same amount of Clevios PH 1000.

PB/PEDOT shows a good performance, with higher cathodic current densities than anodic ones and a short circuit current density even -0.5 mA cm^{-2} higher than the GOPS foil (see Figure 8). An V_{OC} of 0.6 V was reached.

The thickness of the LS/PEDOT foil was not uniformly distributed. To avoid breaking of the electrode during assembling a thicker sample was used, which resulted in higher current densities compared to the foil without any incorporation. However, due to the reason of non-consistent thickness, it was not used for further examinations.

Alizarin/PEDOT resulted in capacitive currents and was therefore not used for further examinations.

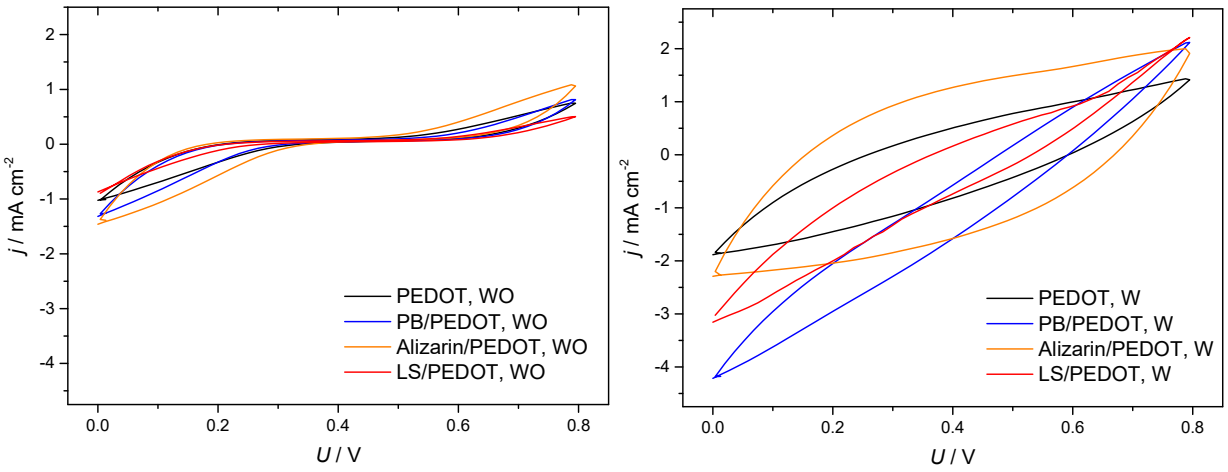

Figure 10: PEDOT:PSS - NFC composite materials with PB (PB/PEDOT), Alizarin (Alizarin/PEDOT) and LS (LS/PEDOT) and PEDOT:PSS - NFC vs Ni: left: 0.05 M HCl without peroxide (WO); right: 0.05 M HCl with 0.1 M peroxide (W)

3.1.5. Electropolymerized PEDOT/ClO_4^-

Electropolymerized PEDOT/ClO_4^- is known for high conductivity. Therefore, it was prepared on FTO, pC and Au substrates. Deposition on FTO was performed under potentiostatic conditions. The deposited film though delaminated quickly from the substrate. Au, pC as well as LS/PEDOT on FTO were prepared under galvanostatic conditions, whereas a deposited film after 900 s showed the best performance. Albeit, only current densities below -1 mA cm^{-2} were achieved which is depicted in Figure 11. However, at 0.4 V a peak appears, which could be due to reduction of hydrogen peroxide and simultaneously oxidation of the catechol group.

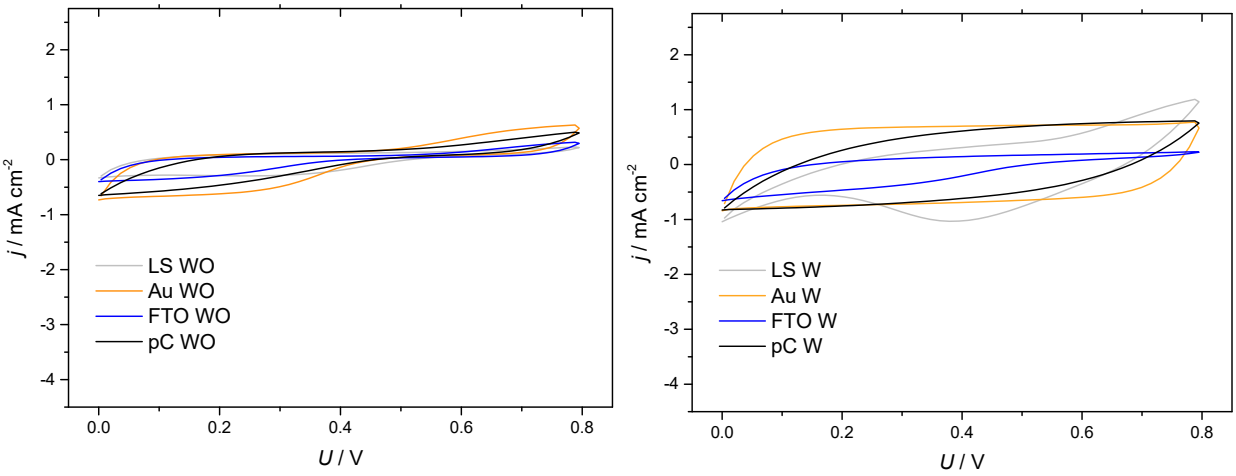

Figure 11: Cyclic voltammograms of electropolymerized PEDOT; copolymerized with LS (LS), polymerized on Au (Au), on FTO (FTO) and on printed Carbon (pC) vs Ni; left: 0.05 M HCl without peroxide (WO); right: 0.05 M with 0.1 M peroxide (W); Au was measured in 0.033 M H_2SO_4; left: without peroxide(WO); right: with 0.1 M peroxide (W)

3.2. Open circuit potential and step chronoamperometry

For further electrochemical examinations PB/PEDOT:PSS - NFC, PEDOT:PSS - NFC (with 1.5 times higher amount) and PEDOT:PSS - GOPS vs Ni were chosen, since their results in the initial measurements were the best.

3.2.1. PB/PEDOT:PSS – NFC

The preliminary results of the PB composite foil were the most promising ones. However, only low current densities and power densities were attained at the step chronoamperometry, which are depicted in Figure 12. Nevertheless, a high open circuit potential of 0.65 V was measured, which is even higher than PB on carbon paper.[11] At 0.3 V a maximum power density of 0.14 mW cm^{-2} was achieved, which is lower to literature values.[11] A j_{SC} of 0.95 mV cm^{-2} was measured, which is more than 3 mA cm^{-2} lower than at the preliminary examinations (see Figure 10).

Unfortunately, the electrode stability was poor. The third measurement already resulted in a decrease of the maximum power density to 0.05 mW cm^{-2}. Moreover, the foil fell apart during the subsequent cleaning procedure with water.

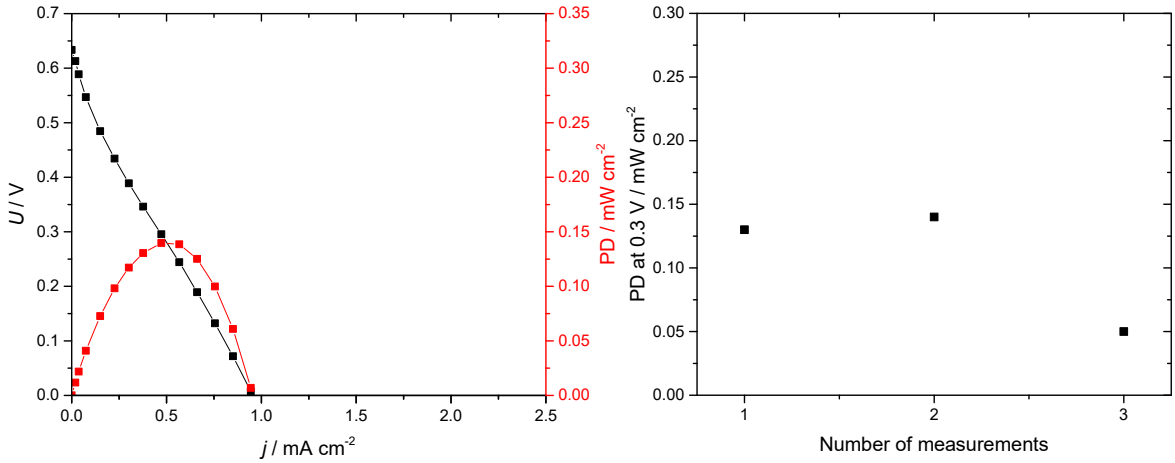

Figure 12: Left: Current density – potential and current density – power density (PD) curves of PB/PEDOT vs Ni in 0.05 M HCl with 0.1 M hydrogen peroxide; Right: Decrease of PD at 0.3 V related to number of measurements

3.2.2. PEDOT:PSS – NFC

PEDOT:PSS – NFC achieved similar results as the PB composite foil, outlined in Figure 13. The V_{OC} is 0.1 V lower, which is approximately at 0.55 V. However, a slightly higher maximum power density of 0.22 mW cm^{-2} at 0.3 V was reached, since activation losses seemed to be lower compared to PB/PEDOT. A short circuit current density of 1.25 mA cm^{-2} was reached.

Also, the stability of the electrode was better compared to PB/PEDOT as the power density decreased only to 0.15 mW cm^{-2} at 0.3 V at the fourth measurement, illustrated in Figure 13.

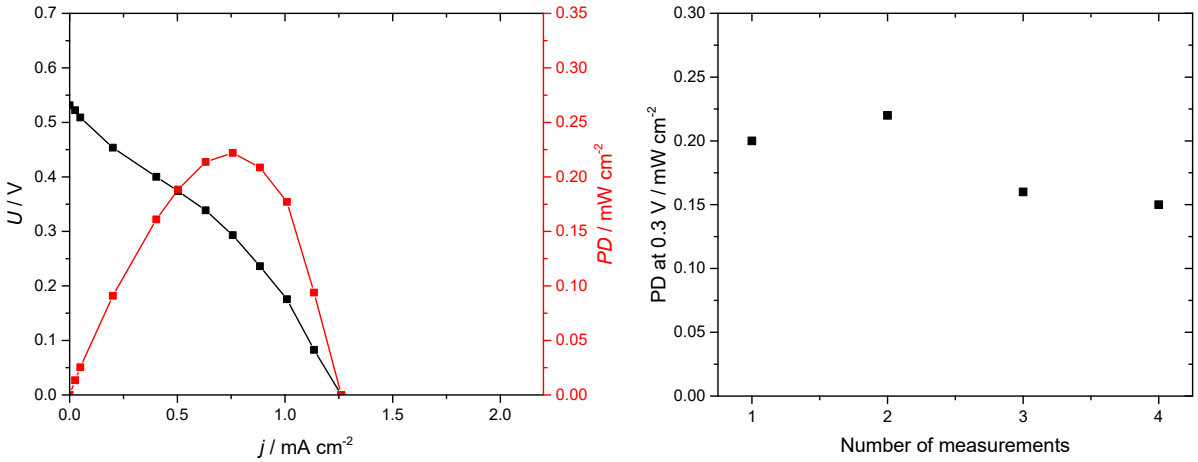

Figure 13: Left: Current density – potential and current density – power density (PD) curves of NFC foil vs Ni in 0.05 M HCl with 0.1 M hydrogen peroxide; Right: Decrease of PD at 0.3 V related to number of measurements

3.2.3. PEDOT:PSS – GOPS

PEDOT:PSS – GOPS showed the best performance as depicted in Figure 14. A maximum power density of 0.30 mW cm^{-2} at 0.25 V was achieved. Also, a higher short circuit current density of 2 mA cm^{-2} was measured. However, this is still 2 mA cm^{-2} lower than determined in the preliminary examinations. Moreover, an V_{OC} of 0.55 V was measured.

Three measurements were performed, which gave similar results. At the fourth measurement the maximum power density decreased to 0.015 mW cm^{-2} at 0.3 V. Yet, the electrode did not fall apart after measurements. A reason for this decrease could be a loss of conductivity, which was already observed at the preliminary tests.

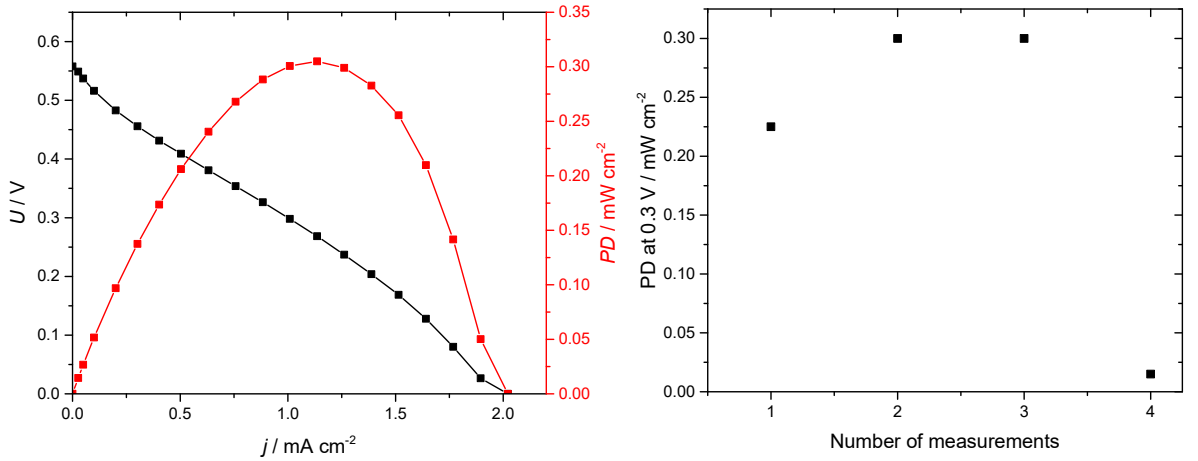

Figure 14: Left: Current density – potential and current density – power density (PD) curves of GOPS foil vs Ni in 0.05 M HCl with 0.1 M hydrogen peroxide; Right: Decrease of PD at 0.3 V related to number of measurements

3.3. Chronopotentiometry at 0V

To investigate the stability of the electrodes in a fuel cell set up, 0 V were applied for several hours. A foil of PEDOT:PSS – GOPS, of PB/PEDOT and of PEDOT:PSS – NFC with a 1.5 times higher amount of Clevios solution compared to the original recipe were chosen for further examinations.

In Figure 15, j_{SC} over time is plotted. On the left side of the figure, the results of three foils are presented for comparison. GOPS reached the highest current density over time, whereas PB/PEDOT decreased the fastest. None of them could maintain a current density over 1 mA cm^{-2} for a long time. Howsoever, even PB on ITO, which is depicted in Figure 15 on the right side, could keep a current density over 1 mA cm^{-2} only for one hour. Afterwards, the performance was similar to the PEDOT foil. However, this experiment would be more informative if the concentration of peroxide was held constant.

PEDOT:PSS (GOPS and NFC) foils decomposed partially during the measurements due to their water solubility. Drop cast PEDOT:PSS - GOPS on FTO was still attached to the substrate. However, the conductivity decreased. Moreover, amber leakage of the PEDOT electrodes was observed, which could be PSS. This phenomenon was observed especially for PEDOT:PSS - NFC, where NFC may replace PSS as counter anion.[17]

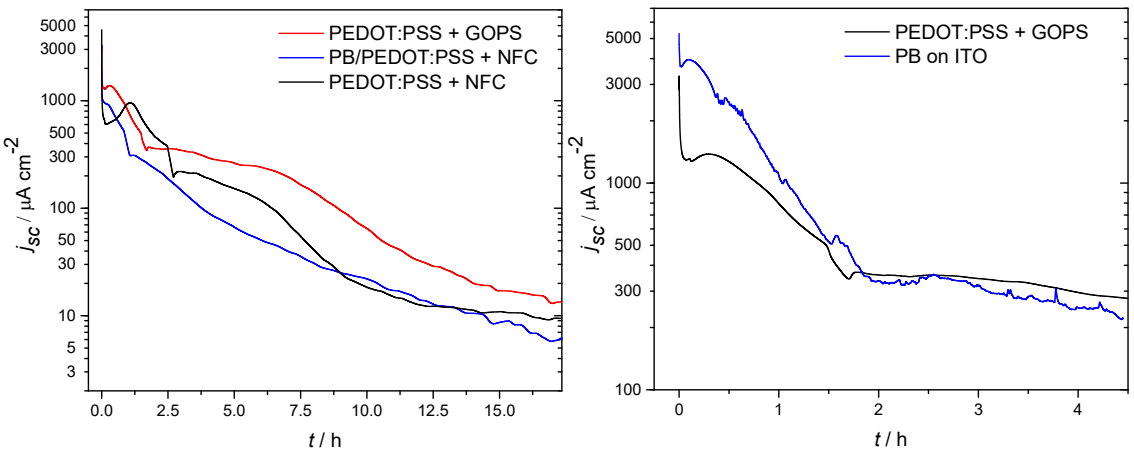

Figure 15: Left: Chronopotentiometric measurements of PEDOT:PSS foils; Right: Comparison with PB on ITO; 0.05 M HCl with 0.1 M hydrogen peroxide was used as electrolyte

3.4. Purging experiments – cyclic voltammetry

To get more insight towards the reaction mechanism of PEDOT and hydrogen peroxide, cyclic voltammetry experiments were performed. They were done under argon, ambient, and oxygen atmosphere in a 3-electrode setup, whereas drop-cast PEDOT:PSS - GOPS was utilized as working electrode, a Ag/AgCl wire as reference, and a Pt mesh as counter electrode. To avoid persistent doping conditions the working electrode was changed between argon purging and ambient experiments. Figure 16 shows the cyclic voltammograms under argon, ambient and oxygen atmosphere in electrolyte without and with 0.1 M peroxide. At WO, PEDOT shows a similar, capacitive behavior under ambient and oxygen purged conditions, whereas under argon atmosphere there are two peaks visible at 0.4 V at the oxidative sweep and at 0.3 V at the reducing sweep. These two peaks could indicate a reversible redox reaction from $PEDOT^0$ to $PEDOT^{2+}$.

In experiments with 0.1 M peroxide (W) the voltammograms for each condition look different. Under ambient conditions, compared to WO conditions, the current density starts to get more negative at around 0.5 V, but only to a value of -1 mA cm^{-2}. This is attributed to the cathodic reduction of H_2O_2 to H_2O. Under O_2 atmosphere the PEDOT electrode behaves similar, with higher cathodic current densities. The higher current is explained by the higher conductivity of the PEDOT electrode, as it is known that oxygen p-dopes PEDOT.[19] Under Ar conditions, the current density starts to get more negative at 0.5 V and further increases to around -5 mA cm^{-2} at about 0.1 V. Then there is a plateau like behavior until -0.1 V. Afterwards, again an increase to -5.5 mA cm^{-2} is observed. At the oxidative sweep, the current density gets positive again until a plateau-like behavior with a current density of 1.5 mA cm^{-2} at 0.5 V is reached. This substantial increase in the current under H_2O_2 and Ar purging conditions are attributed to the redox cycle whereby dedoped $PEDOT^{(0)}$ is oxidized by H_2O_2 and then in turn the PEDOT is reduced again due to the cathodic polarization. This redox cycle is maximized when the starting conditions feature dedoped $PEDOT^{(0)}$ which can react with H_2O_2. This redox cycle which is illustrated in Figure 16 is referred to be responsible for the function of PEDOT as a suitable peroxide fuel cell cathode.

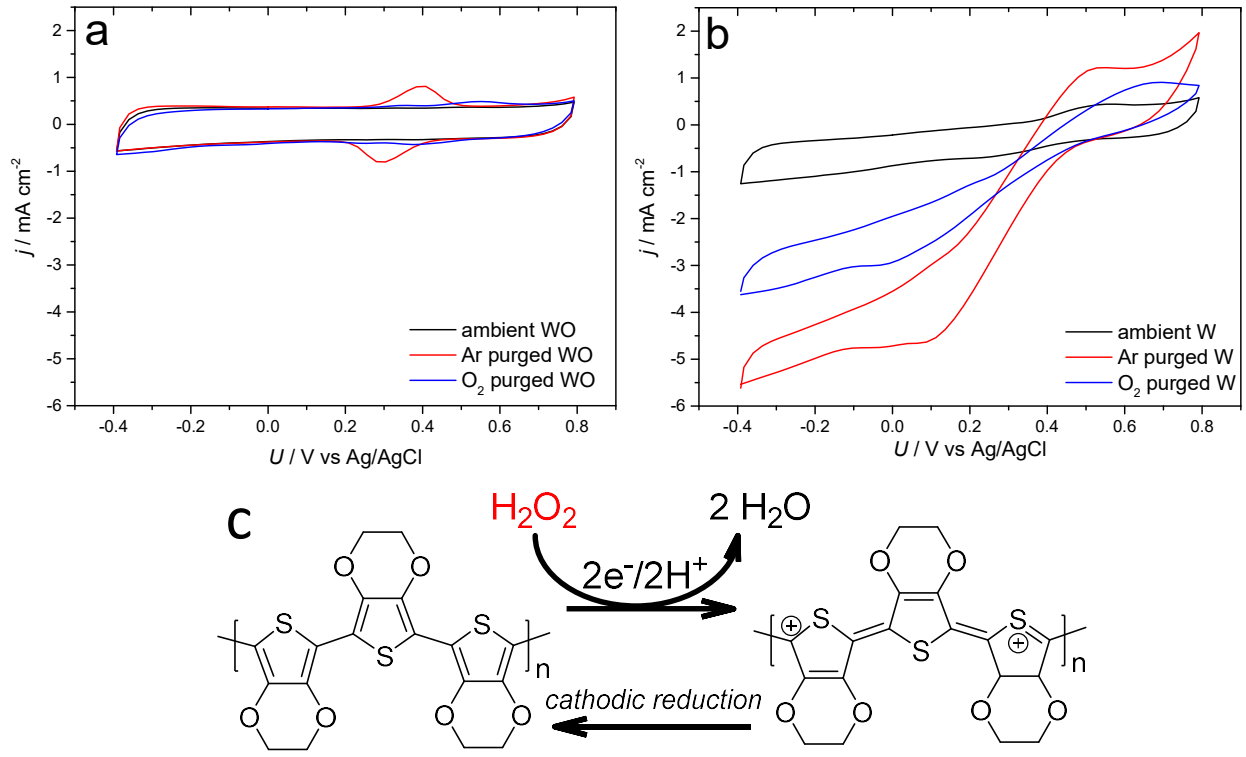

Figure 16: Cyclic voltammograms of PEDOT:PSS – GOPS under Ar purged, ambient and oxygen purged conditions: a) 0.05 M HCl without peroxide (WO); b) 0.05 M HCl with 0.1 M peroxide (W); c) mechanism of PEDOT redox cycle

Afterwards, measurements of the used electrodes for Ar and O_2 purging experiments were performed in a single compartment fuel cell set up, depicted in Figure 17. It was observed that the short circuit current densities were in the case of Ar purging (c) almost 2 mA cm^{-2} and in the case of O_2 purging (b) about 1.25 mA cm^{-2} higher compared to electrodes, which were only used at ambient conditions (a). The V_{OC} however did not change. Thus Ar-treated electrodes are pre-dedoped and give higher initial current density.

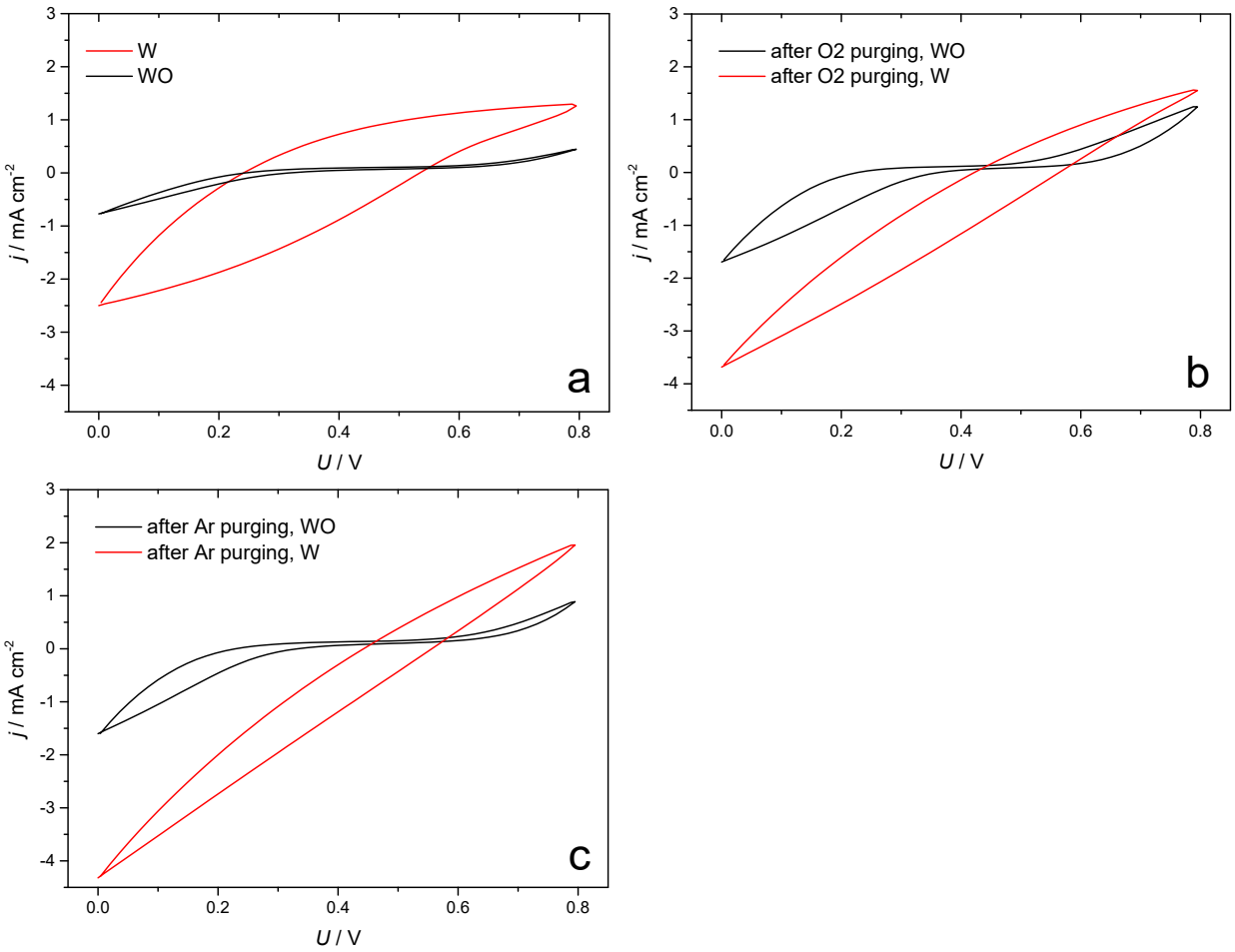

Figure 17: Cyclic voltammograms of PEDOT:PSS – GOPS vs Ni in a fuel cell set up: a) under ambient conditions; b) after oxygen purging; c) after argon purging; 0.05 M HCl without peroxide (WO) and with 0.1 M peroxide (W)

3.5. Testing the disproportionation reaction of hydrogen peroxide on catalyst materials

As gas evolution was observed on electrode material surfaces the decomposition of hydrogen peroxide was investigated. Disproportionation of peroxide is considered a loss mechanism for the fuel cell, as the fuel decomposes without giving electrical current. To gain results two different methods were applied, the UV-vis direct assay and the horseradish peroxidase / TMB assay (HRP assay).

In general, the disproportionation reaction of hydrogen peroxide proceeds as follows:[4]

$$2\ H_2O_2 \rightarrow 2\ H_2O + O_2 \qquad (4)$$

Since surface reactions with the different materials are involved the exact decomposition reactions are unknown. For rate determination, time vs concentration of hydrogen peroxide was plotted. Then, a linear fit was added and its slope was assumed to be the rate.

3.5.1. UV vis – direct assay

Drop-cast PEDOT:PSS - NFC on FTO (NFC), Prussian Blue on ITO (PB) and a Ni – mesh (Ni), each immersed into electrolyte solution, as well as one sample without any catalyst immersed (blank) were measured.

As plotted in Figure 18 PB and Ni tend to decompose, while PEDOT:PSS - NFC produces peroxide. The change of concentration of the blank sample was treated as measuring inaccuracy. In Table 5 the average hydrogen peroxide concentrations of both evaluated wavelengths and corresponding decomposition rates are shown. The decomposition rate of peroxide at the Ni electrode is about 2 mM h^{-1}; for PB only 0.3 mM h^{-1}, which may be negligible.

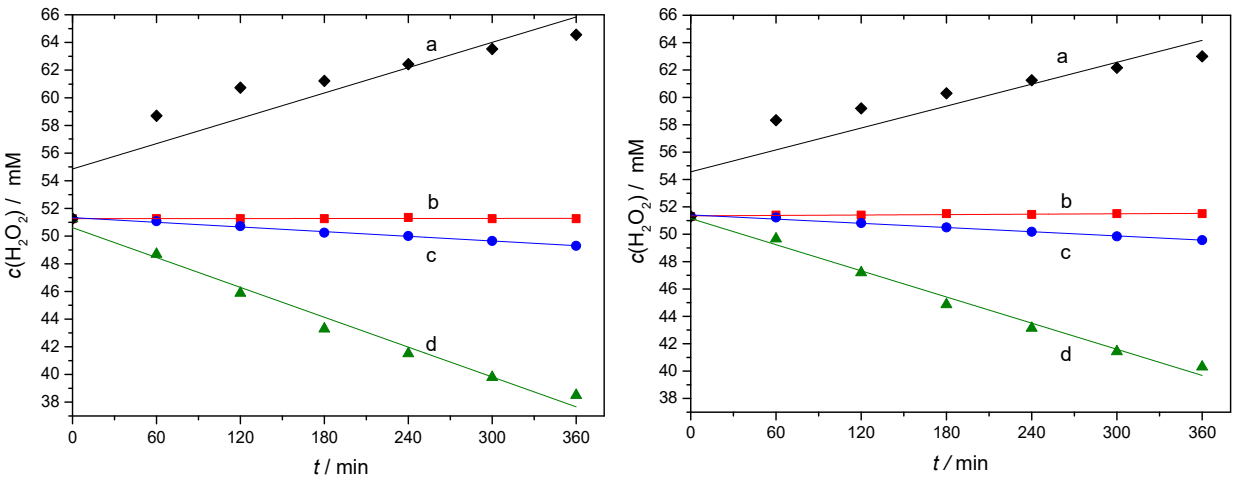

Figure 18 : Direct assay; time vs perox ide concentration with linear fit: left: at 240 nm, (a) NFC (b) blank (c) PB (d) Ni; right; at 250 nm, (a) NFC (b) blank (c) PB (d) Ni

Table 5: Average concentration of hydrogen peroxide of 240 and 250 nm and corresponding average rate of decomposition for different materials according to direct assay

Time / h	$c(H_2O_2)$ / mM			
	Blank	**PB**	**NFC**	**Ni**
0	51.3	51.3	51.3	51.3
1	51.3	51.2	58.5	49.2
2	51.3	50.8	60.0	46.5
3	51.4	50.4	60.8	44.1
4	51.4	50.1	61.8	42.3
5	51.4	49.8	62.9	40.6
6	51.4	49.4	63.8	39.4
Rate / mM h^{-1}	0.021	-0.322	1.716	-2.035

To evaluate if PEDOT:PSS is indeed producing 1.7 mM peroxide per hour, samples (NFC and GOPS) were immersed into solutions without peroxide and measured in the beginning and after six hours. Apparently, the spectra change (see Figure 19), which could possibly be due to leakage of PSS.

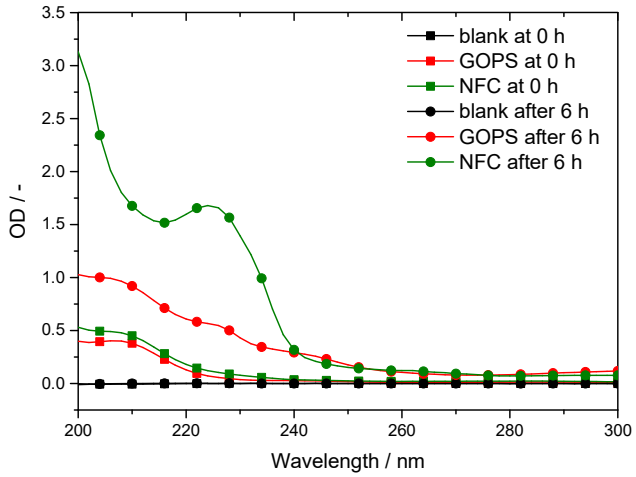

Figure 19: Spectra of PEDOT (GOPS and NFC) electrodes in 0.05 M HCl; after 0 and after 6 hours

To be sure, if PSS leakage caused the change of optical density and not hydrogen peroxide production, another peroxide assay was applied additionally to provide more realistic results.

3.5.2. HRP assay

Prussian blue on ITO, a Ni-mesh, a foil of PEDOT:PSS – NFC as well as a foil of PEDOT:PSS - GOPS and a blank sample were measured as described in the experimental part.

In Figure 20 and Table 6 the results are represented. They show similar fluctuations for the PEDOT:PSS - NFC and PB samples compared to the blank one. Therefore, it can be said that neither hydrogen peroxide is produced nor decomposed in a significant amount. Also, this can be said for PEDOT:PSS – GOPS. However, the fluctuations are less significant.

Ni shows a similar behavior as in the direct assay. Hence it is clear that decomposition of peroxide happens on the Ni-mesh.

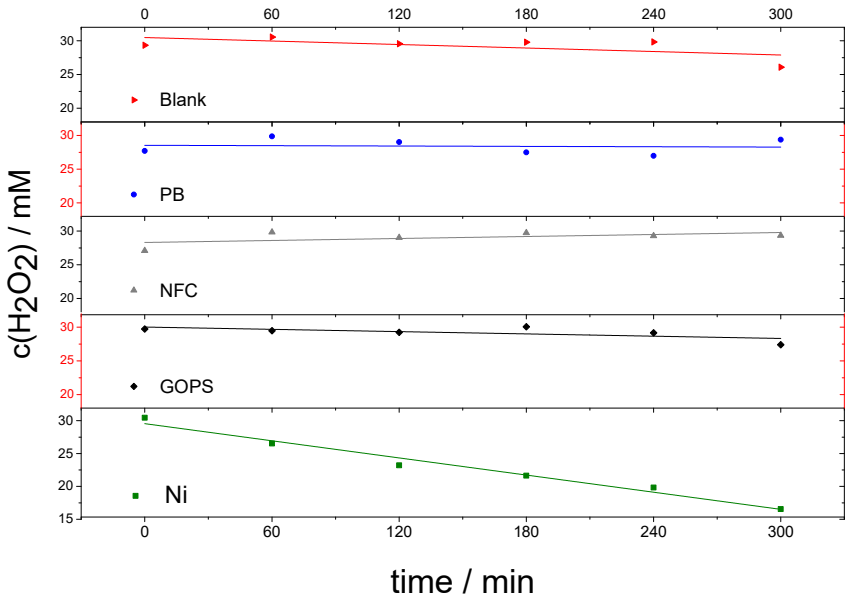

Figure 20: HRP assay of Blank, PB, PEDOT:PSS – NFC, PEDOT:PSS – GOPS and Ni, time vs hydrogen peroxide concentration with linear fit

Table 6: Concentration of hydrogen peroxide and rate of decomposition for different materials according to HRP assay

Time / h	$c(H_2O_2)$ / mM				
	Blank	**PB**	**NFC**	**GOPS**	**Ni**
0	29.3	27.7	27.1	29.7	30.5
1	30.5	29.9	29.8	29.5	26.5
2	29.6	29.0	29.0	29.2	23.2
3	29.8	27.5	29.7	30.0	21.6
4	29.8	27.0	29.3	29.1	19.8
5	26.1	29.4	29.3	27.4	16.5
Rate / mM h^{-1}	-0.511	-0.049	0.291	-0.340	-2.620

To provide clarification for PB and PEDOT:PSS - NFC samples, they were measured again, which can be seen in Figure 21. These results of the second measurement outlined in Table 7 show low decomposition rates for NFC and PB whereas for the blank sample a slight increase of peroxide is measured.

If the average decomposition rates of those two measurements, as shown in Table 8, are compared it could be interpreted, that since they are very low they either even stabilize hydrogen peroxide in the solution or changes can be neglected.

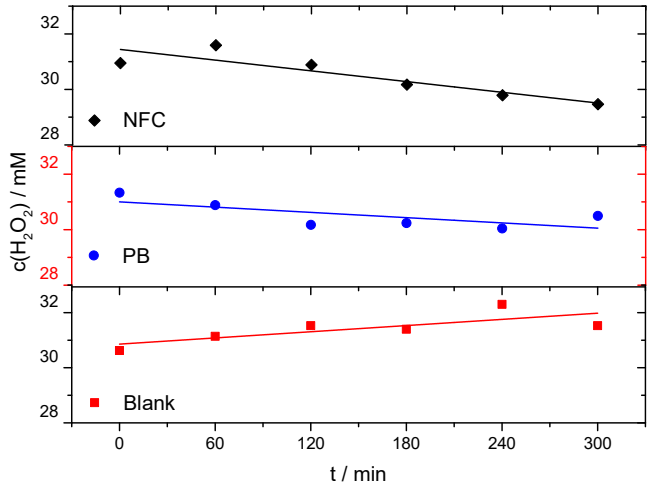

Figure 21: Repetition of HRP assay of PB on ITO, PEDOT:PSS – NFC foil and blank, time vs hydrogen peroxide concentration

Table 7: Concentration of hydrogen peroxide and rate of decomposition for blank, PB and PEDOT:PSS - NFC according to HRP assay

Time / h	$c(H_2O_2)$ / mM		
	Blank	PB	NFC
0	30.6	31.3	30.9
1	31.1	30.9	31.6
2	31.5	30.2	30.9
3	31.4	30.2	30.2
4	32.3	30.0	29.8
5	31.5	30.5	29.5
Rate / mM h^{-1}	0.229	-0.194	-0.374

Table 8: Average decomposition rate of Hydrogen Peroxide for blank, Prussian blue (PB) and PEDOT:PSS – NFC (NFC) samples

Measurement	Blank / mM h^{-1}	PB / mM h^{-1}	NFC / mM h^{-1}
1	-0.511	-0.049	0.291
2	0.229	-0.194	-0.374
Average rate	-0.141	-0.122	-0.083

3.6. Anode catalysts

Ni tends to decompose hydrogen peroxide without generating power (see chapter 'Testing the disproportionation reaction of hydrogen peroxide on catalyst materials' and Yamazaki et al. [5]) as well as to corrode in the acidic electrolyte. Moreover, as Ni^{2+} it is toxic, and also forms complexes with water molecules which can be observed as the color of the electrolyte changes from colorless to greenish. Therefore, it is advantageous to search for an anodic catalyst which is stable and does not induce disproportionation.

Hence, several catalyst materials were tested in a single compartment fuel cell, where PB on ITO or PEDOT:PSS were utilized as cathode. However, all investigated materials show only low electrocatalytic activity towards oxidation of peroxide and are therefore not considered promising. The measured current densities were in the µA cm^{-2} range.

Tested materials were TCNQ on FTO, thermally oxidized Ti, PTCDI on Au, PEDOT:PSS, QNC on Au and SA-3 on pC.

Yet, it was found that the stability of Ni was improved when it was thermally oxidized (500 ˚C) for 15 minutes before measurements, producing a NiO surface layer. Chronoamperometric measurements, see Figure 22, show that for PB on ITO vs oxidized Ni a short circuit current density over 1 mA cm^{-2} is maintained for about 3 hours which is 2 hours longer compared to PB on ITO vs untreated Ni. Neither was the oxidized Ni corroded nor did the color of the electrolyte change.

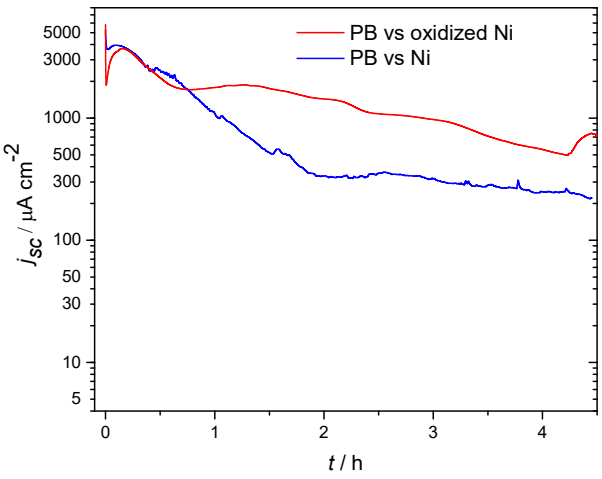

Figure 22: Chronoamperometric measurements at 0 V of PB vs oxidized Ni and untreated Ni in 0.05 M HCl with 0.1 M peroxide

4. Conclusion and further outlook

In this work it was shown that PEDOT:PSS electrodes can be applied as cathode materials vs Ni for single compartment hydrogen peroxide fuel cells, although the obtained power density did not reach the currently highest value of 4.2 mW cm^{-2}.[14] Still, an open circuit potential of 0.6 V was achieved, which is competitive with other investigated cathode catalysts. However, the stability of the foils was poor and therefore is needed to be improved. Nevertheless, decomposition of peroxide at PEDOT surfaces does not occur. GOPS improves the stability in the electrolyte, however a decrease of conductivity is observed, while NFC ensures conductivity but increases swelling and solubility.

Concerning the composite electrodes, PB is likely to improve the performance if well dispersed mixtures could be obtained. On the contrary, alizarin and LS did not show the desired effect of the redox reaction of the catechol group.

Unfortunately, there was no success to find a substitution for Ni. However, oxidized Ni seemed to be more stable as well as higher current densities were obtained. Further investigations concerning disproportionation of hydrogen peroxide and performance tests could be interesting.

List of Tables

List of Figures

References

(1) Dai, L.; Xue, Y.; Qu, L.; Choi, H. J.; Baek, J. B. Metal-Free Catalysts for Oxygen Reduction Reaction. *Chem. Rev.* **2015**, *115* (11), 4823–4892.

(2) Yamada, Y. Electrocatalysts for Hydrogen Peroxide Reduction Used in Fuel Cells; *Anion Exchange Membrane Fuel Cells*, An, L., Zhao, T. S., Eds.; Springer International Publishing, **2018,** 141-168

(3) Mase, K.; Yoneda, M.; Yamada, Y.; Fukuzumi, S. Seawater Usable for Production and Consumption of Hydrogen Peroxide as a Solar Fuel. *Nat. Commun.* **2016**, *7* (May), 11470.

(4) Goor, G.; Glenneberg, J.; Jacobi, S. Hydrogen Peroxide. *Ullmann's Encyclopedia of Industrial Chemistry*; **2011**; Vol. 18, pp 393–427.

(5) Yamazaki, S.; Siroma, Z.; Senoh, H.; Ioroi, T.; Fujiwara, N.; Yasuda, K. A Fuel Cell with Selective Electrocatalysts Using Hydrogen Peroxide as Both an Electron Acceptor and a Fuel. *J. Power Sources* **2008**, *178* (1), 20–25.

(6) Kato, S.; Jung, J.; Suenobu, T.; Fukuzumi, S. Production of Hydrogen Peroxide as a Sustainable Solar Fuel from Water and Dioxygen. *Energy Environ. Sci.* **2013**, *6* (12), 3756–3764.

(7) Jakešová, M.; Apaydin, D. H.; Sytnyk, M.; Oppelt, K.; Heiss, W.; Sariciftci, N. S.; Głowacki, E. D. Hydrogen-Bonded Organic Semiconductors as Stable Photoelectrocatalysts for Efficient Hydrogen Peroxide Photosynthesis. *Adv. Funct. Mater.* **2016**, *26* (29), 5248–5254.

(8) Warczak, M.; Gryszel, M.; Jakesova, M.; Derek, V.; Głowacki, E. D. Organic Semiconductor Perylenetetracarboxylic Diimide (PTCDI) Electrodes for Electrocatalytic Reduction of Oxygen to Hydrogen Peroxide. *Chem. Commun.* **2018**, *54* (16), 1960–1963.

(9) Gryszel, M.; Sytnyk, M.; Jakesova, M.; Romanazzi, G.; Gabrielsson, R.; Heiss, W.; Głowacki, E. D. General Observation of Photocatalytic Oxygen Reduction to Hydrogen Peroxide by Organic Semiconductor Thin Films and Colloidal Crystals. *ACS Appl. Mater. Interfaces* **2018**, *10* (16), 13253–13257.

(10) Campos-Martin, J. M.; Blanco-Brieva, G.; Fierro, J. L. G. Hydrogen Peroxide

Synthesis: An Outlook beyond the Anthraquinone Process. *Angew. Chemie - Int. Ed.* **2006**, *45* (42), 6962–6984.

(11) Mousavi Shaegh, S. A.; Nguyen, N.-T.; Mousavi Ehteshami, S. M.; Chan, S. H. A Membraneless Hydrogen Peroxide Fuel Cell Using Prussian Blue as Cathode Material. *Energy Environ. Sci.* **2012**, *5* (8), 8225–8228.

(12) Yamada, Y.; Fukunishi, Y.; Yamazaki, S.; Fukuzumi, S. Hydrogen Peroxide as Sustainable Fuel: Electrocatalysts for Production with a Solar Cell and Decomposition with a Fuel Cell. *Chem. Commun.* **2010**, *46* (39), 7334–7336.

(13) Yamada, Y.; Yoshida, S.; Honda, T.; Fukuzumi, S. Protonated Iron–phthalocyanine Complex Used for Cathode Material of a Hydrogen Peroxide Fuel Cell Operated under Acidic Conditions. *Energy Environ. Sci.* **2011**, *4* (8), 2822–2825.

(14) Yamada, Y.; Yoneda, M.; Fukuzumi, S. High Power Density of One-Compartment H_2O_2 Fuel Cells Using Pyrazine-Bridged $Fe[M^C(CN)_4]$(M^C =Pt^{2+} and Pd^{2+}) Complexes as the Cathode. *Inorg. Chem.* **2014**, *53*, 1272–1274.

(15) Kirchmeyer, S.; Reuter, K. Scientific Importance, Properties and Growing Applications of Poly(3,4-Ethylenedioxythiophene). *J. Mater. Chem.* **2005**, *15* (21), 2077–2088.

(16) Groenendaal, L.; Jonas, F.; Freitag, D.; Pielartzik, H.; Reynolds, J. R. Poly(3,4-Ethylenedioxythiophene) and Its Derivatives : Past , Present , and Future **. *Adv. Mater.* **2000**, *12* (7), 481–494.

(17) Malti, A.; Edberg, J.; Granberg, H.; Khan, Z. U.; Andreasen, J. W.; Liu, X.; Zhao, D.; Zhang, H.; Yao, Y.; Brill, J. W.; et al. An Organic Mixed Ion-Electron Conductor for Power Electronics. *Adv. Sci.* **2015**, *3* (2).

(18) Winther-Jensen, B.; Winther-Jensen, O.; Forsyth, M.; MacFarlane, D. R. High Rates of Oxygen Reduction. *Science (80-.).* **2008**, *321*, 671–674.

(19) Mitraka, E.; Jafari, M. J.; Vagin, M.; Liu, X.; Fahlman, M.; Ederth, T.; Berggren, M.; Jonsson, M. P.; Crispin, X. Oxygen-Induced Doping on Reduced PEDOT. *J. Mater. Chem. A* **2017**, *5* (9), 4404–4412.

(20) Sun, K.; Zhang, S.; Li, P.; Xia, Y.; Zhang, X.; Du, D.; Isikgor, F. H.; Ouyang, J.

Review on Application of PEDOTs and PEDOT:PSS in Energy Conversion and Storage Devices. *J. Mater. Sci. Mater. Electron.* **2015**, *26* (7), 4438–4462.

(21) Wang, J.; Wang, Y.; Cui, M.; Xu, S.; Luo, X. Enzymeless Voltammetric Hydrogen Peroxide Sensor Based on the Use of PEDOT Doped with Prussian Blue Nanoparticles. *Microchim. Acta* **2017**, *184* (2), 483–489.

(22) Siao, H. W.; Chen, S. M.; Lin, K. C. Electrochemical Study of PEDOT-PSS-MDB-Modified Electrode and Its Electrocatalytic Sensing of Hydrogen Peroxide. *J. Solid State Electrochem.* **2011**, *15* (6), 1121–1128.

(23) Hakimi, M.; Salehi, A.; Boroumand, F. A. Experimental Study on PEDOT : PSS Conductive Polymer and N-Doped Graphene Quantum Dots for H_2O_2 Sensing. *Bull. la Société R. des Sci. Liège* **2016**, *85*, 261–268.

(24) Karyakin, A. A. Advances of Prussian Blue and Its Analogues in (Bio)Sensors. *Curr. Opin. Electrochem.* **2017**, *5* (1), 92–98.

(25) Asadnia, M.; Mousavi Ehteshami, S. M.; Chan, S. H.; Warkiani, M. E. Development of a Fiber-Based Membraneless Hydrogen Peroxide Fuel Cell. *RSC Adv* **2017**, *7* (65), 40755–40760.

(26) Karpova, E. V.; Karyakina, E. E.; Karyakin, A. A. Iron–nickel Hexacyanoferrate Bilayer as an Advanced Electrocatalyst for H_2O_2 Reduction. *RSC Adv.* **2016**, *6* (105), 103328–103331.

(27) Young, J. A. Catechol. *J. Chem. Educ. Today* **2005**, *82* (1), 31.

(28) Nematollahi, D.; Rafiee, M. Electrochemical Oxidation of Catechols in the Presence of Acetylacetone. *J. Electroanal. Chem.* **2004**, *566* (1), 31–37.

(29) Jeliński, T.; Cysewski, P. Structure and Properties of Alizarin Complex Formed with Alkali Metal Hydroxides in Methanol Solution. *J. Mol. Model.* **2016**, *22* (6), 126.

(30) de Fátima Cardoso Soares, M.; de Oliveira Farias, E. A.; da Silva, D. A.; Eiras, C. Development and Characterization of Hybrid Films Based on Agar and Alizarin Red S for Applications as Non-Enzymatic Sensors for Hydrogen Peroxide. *J. Mater. Sci.* **2016**, *51* (15), 7093–7107.

(31) Han, H.; Wu, X.; Wu, S.; Zhang, Q.; Lu, W.; Zhang, H.; Pan, D. Fabrication of

Alizarin Red S/Multi-Walled Carbon Nanotube Nanocomposites and Their Application in Hydrogen Peroxide Detection. *J. Mater. Sci.* **2013**, *48* (9), 3422–3427.

(32) Ręþiś, T.; Milczarek, G. A Comparative Study on the Preparation of Redox Active Bioorganic Thin Films Based on Lignosulfonate and Conducting Polymers. *Electrochim. Acta* **2016**, *204*, 108–117.

(33) Ajjan, F. N.; Casado, N.; Rębiś, T.; Elfwing, A.; Solin, N.; Mecerreyes, D.; Inganäs, O. High Performance PEDOT/Lignin Biopolymer Composites for Electrochemical Supercapacitors. *J. Mater. Chem. A* **2016**, *4* (5), 1838–1847.

(34) Edberg, J.; Inganäs, O.; Engquist, I.; Berggren, M. Boosting the Capacity of All-Organic Paper Supercapacitors Using Wood Derivatives. *J. Mater. Chem. A* **2018**, *6* (1), 145–152.

(35) Garcia-Jareno, J. J.; Benito, D.; Navarro-Laboulais, J.; Vicente, F. Electrochemical Behavior of Electrodeposited Prussian Blue Films on ITO Electrode: An Attractive Laboratory Experience. *J. Chem. Educ.* **1998**, *75* (7), 881–884.

(36) Håkansson, A.; Han, S.; Wang, S.; Lu, J.; Braun, S.; Fahlman, M.; Berggren, M.; Crispin, X.; Fabiano, S. Effect of (3-Glycidyloxypropyl)Trimethoxysilane (GOPS) on the Electrical Properties of PEDOT:PSS Films. *J. Polym. Sci. Part B Polym. Phys.* **2017**, *55* (10), 814–820.